

## Electron microscopy of NPL crystallites in a thermotropic random copoly(ester-amide)

Richard J. Spontak\* and Alan H. Windle†

Department of Materials Science and Metallurgy, University of Cambridge, Pembroke Street, Cambridge CB2 3QZ, UK

(Received 25 May 1989; revised 28 September 1989; accepted 28 September 1989)

The crystalline features of a thermotropic copoly(ester-amide) are investigated with transmission electron microscopy (TEM). Selected-area electron diffraction patterns reveal that the meridional maxima are aperiodic, indicating that the molecular sequencing of the copolymer is random, and that annealing significantly increases the local molecular orientation. The specimens also exhibit non-periodic layer (NPL) crystallites, measuring approximately 15 nm thick and 90 nm long (as imaged in the principal equatorial reflection) and oriented with their thin axis parallel to the molecular axis. Imaging of crystallites in both bright field and dark field, using the meridional maxima as sources of diffraction contrast, has been possible due to the diffraction intensity of the crystallites and the radiation stability of the material, whose mean saturation dose is of the order of 470 C/m<sup>2</sup>.

(Keywords: NPL crystallites; liquid crystalline polymers; thermotropic random copolymers; transmission electron microscopy; polymer microstructure)

### INTRODUCTION

In a recent work<sup>1</sup>, the characteristics and morphology of non-periodic layer (NPL) crystallites in both high and low molecular weight thermotropic copolyesters composed of 4-hydroxybenzoic acid (HBA) and 2-hydroxy-6-naphthoic acid (HNA) residues have been investigated using dark-field (DF) imaging in transmission electron microscopy (TEM). These copolymers have been shown previously to possess random molecular sequencing from X-ray diffraction patterns<sup>2-5</sup>. The crystallites, such as the one illustrated in *Figure 1*, are the result of longitudinal register between adjacent, identical sequences of monomer units and appear oriented with their thin axis aligned parallel to the molecular axis.

The size of these crystalline entities depends on a variety of factors, such as molecular composition, molecular weight (or degree of polymerization, *DP*), and thermal history, with the *DP* being the most influential factor. In the high molecular weight HBA/HNA materials, possessing an approximately constant *DP* ( $\approx 150$ ), the crystallites are of the order of 20 nm thick and 40–100 nm long, depending on composition and thermal history<sup>1</sup>, and are similar to those first reported<sup>6</sup>. However, the largest crystallites in a low molecular weight 75/25 HBA/HNA copolymer (*DP*  $\approx 25$ ) have been shown to be approximately 300 nm long<sup>1,7</sup>. This order of length has also been verified in chemically etched samples with scanning electron microscopy (SEM)<sup>8</sup>.

The purpose of the present work is to report the characteristics of NPL crystallites occurring in a closely related, but chemically different, thermotropic random copolymer. The presence of such crystallites in this material suggests that these crystalline entities may be present in a variety of similar materials.

### EXPERIMENTAL

The material used in this study was Vectra B9000, manufactured by the Hoechst-Celanese Corporation (Summit, NJ, USA). It belongs to the same family of thermotropic copolymers as the HBA/HNA copolyesters. Although the composition and molecular weight of this copoly(ester-amide) presently constitute proprietary information, elemental analysis of the material suggests that 18.6% of the spacer linkages are amide instead of ester. If we were to assume that the polymer is based on HNA, terephthalic acid (TH), and hydroquinone (HQ), then the chemical analysis would be consistent with an HNA content of around 60%, and the 20% HQ being substituted to a very significant extent (>85%) by hydroxylaniline (HA) units. For brevity, this class of copolymer will hereafter be referred to as N-AT.

Ultrathin films of this material, suitable for TEM investigation, were prepared according to the method provided in detail elsewhere<sup>1</sup>. Small blocks were cut from the centre of an extruded rod measuring 18 mm in

```
A A A A A A
B B B B B B
B B B B B B
A A A A A A
A A A A A A
A A A A A A
B B B B B B
A A A A A A
B B B B B B
B B B B B B
B B B B B B
A A A A A A
```

**Figure 1** Illustration of a non-periodic layer (NPL) crystallite in a random copolymer, in which A and B refer to the monomer species present. The crystallites are the result of lateral sequencing of like monomers in adjacent chains, whose molecular axis is vertical

\* Present address: Department of Physics, Institute for Energy Technology, PO Box 40, N-2007 Kjeller, Norway

† To whom correspondence should be addressed

diameter. Each block was placed on freshly cleaved rock salt and heated to 310°C, which is above the temperature at which the viscosity of the copolymer dramatically decreases and the material becomes a birefringent melt. (This temperature was found by differential scanning calorimetry (d.s.c.), operated at 20°/min in an inert nitrogen atmosphere, to be about 271°C.) While in its fluid mesophase, the molten sample was quickly sheared and quenched to 0°C on an aluminium block. Upon dissolution of the rock salt, the remaining ultrathin films were picked up on folding grids and, unless otherwise stated, annealed for 60 min at 250°C, followed by carbon coating to increase stability under the electron beam.

A Jeol JEM 2000-EX electron microscope, operated at 200 keV and fitted with a LaB<sub>6</sub> filament and high resolution pole piece, was used throughout this study. Relevant information regarding the optical system of the microscope<sup>1</sup> and the procedures to minimize contamination and beam damage have already been provided. Microdensitometry was accomplished using a Joyce-Loebl digital scanning microdensitometer (Technical Operations, Inc., Burlington, MA, USA) set on a 25 μm spot size. Image enhancement of the resultant 512 × 512 pixel arrays utilized the Semper VI algorithm by Synoptics Ltd.

## RESULTS AND DISCUSSION

### Imaging modes

Selected area electron diffractograms (SAEDs) from a region approximately 2.5 μm in diameter are presented in Figure 2. Figure 2a was obtained from an unannealed film. Arced equatorial and meridional reflections are reminiscent of the SAEDs obtained from HBA/HNA copolymers<sup>1,7,9</sup>. The ratio of scattering vectors between the two meridional maxima is 0.28, indicating that the maxima are aperiodic and that the copolymer is indeed

random. In comparison, an SAED from an annealed specimen is presented in Figure 2b. The diffraction peaks show less arcing than those in Figure 2a and suggest a more highly oriented material.

A schematic illustration of the SAED is presented in Figure 3. The overlaid circles represent the position of the objective aperture in the electron microscope. Positioning the aperture over the centre spot (B in Figure 3) results in bright-field (BF) imaging, in which contrast is due primarily to thickness variations or compositional heterogeneity. Imaging in DF depends on diffraction contrast and is obtained by tilting the electron beam so that a region of the SAED, other than the centre spot,

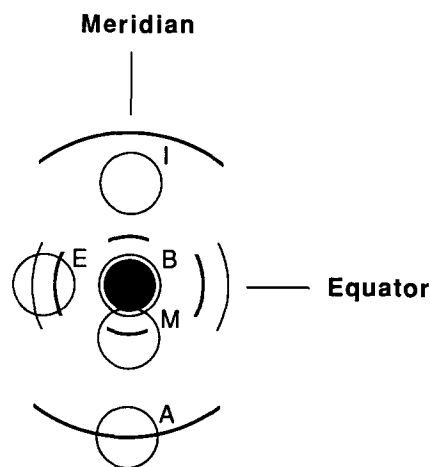


Figure 3 Schematic diagram of the SAED shown in Figure 2. The superimposed circles represent the position of the objective aperture in the electron microscope, with bright-field (BF) imaging resulting when the aperture is over the beam centre spot (B). Dark-field (DF) imaging utilizes other regions of the SAED and includes the equatorial reflection (E), the first meridional maximum (M), the intrachain region between the meridional maxima (I), and the broad meridional arc (A)

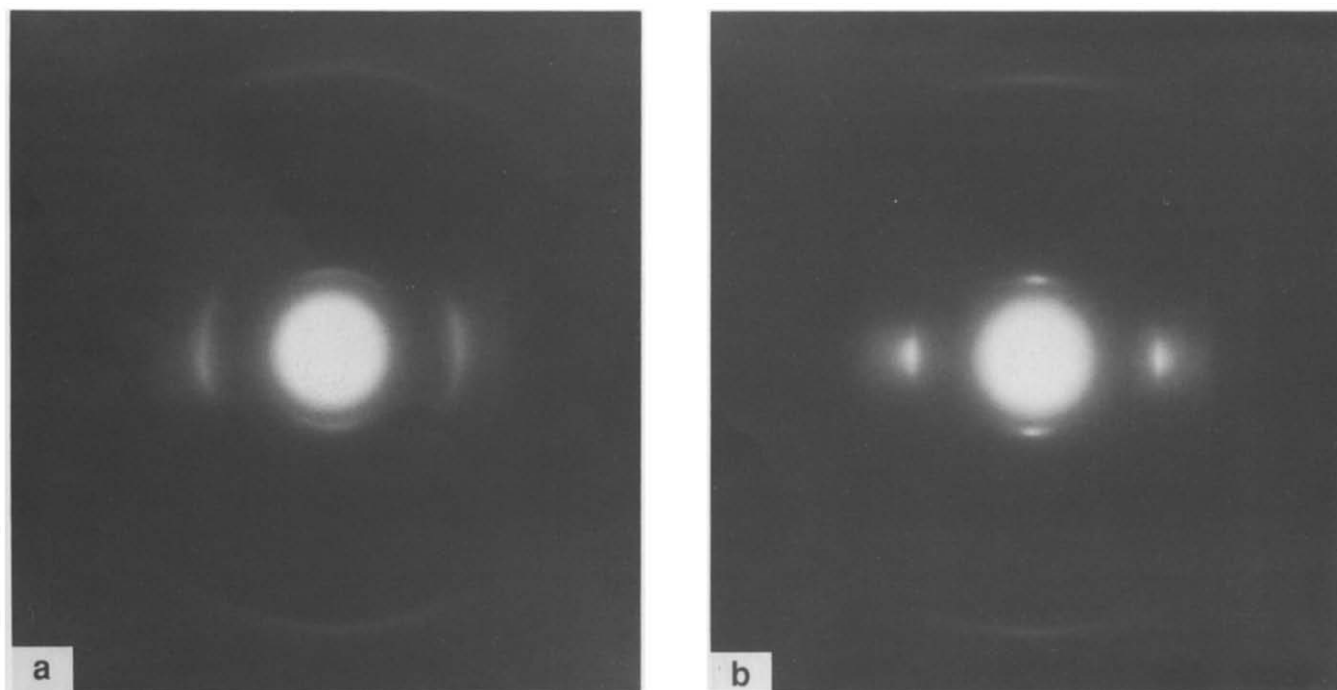


Figure 2 Selected-area electron diffractograms (SAEDs) of the N-AT copolymer. SAEDs from both the unannealed (a) and annealed (b) samples exhibit aperiodic meridional maxima, indicating that the molecular sequencing is random. The annealed material (b) appears more oriented than its unannealed analogue (a)

is located in the aperture. In this work, imaging has been accomplished in four different regions of the SAED: the principal equatorial reflection (E), the first meridional spot (M), the 'intrachain' region between the meridional maxima (I), and the broad meridional arc (A).

A BF/DF pair of electron micrographs of an identical region of the specimen is displayed in *Figure 4*. The DF micrograph (*Figure 4a*) is imaged in the equatorial reflections and clearly shows the presence of diffracting entities, measuring about 15 nm thick and 90 nm long. These are very similar to the NPL crystallites seen in HBA/HNA copolymers (which are 20 nm in thickness and 40–100 nm in length for high molecular weight materials<sup>1,6</sup> and 10 nm in thickness and up to 300 nm in length for a low molecular weight analogue<sup>1,7</sup>). As with all of the micrographs presented in this work, the shear direction, i.e., the molecular axis<sup>10</sup>, is kept vertical. It is clear from *Figure 4a* that the crystallites are oriented with their thin axis parallel to the molecular axis. Dark entities, corresponding closely to the size and distribution of the crystallites seen in DF, are apparent in the BF image of the same area (*Figure 4b*). It should be borne in mind that the number of crystallites seen in *Figure 4b* is likely to be less than that in *Figure 4a* due to radiation damage.

Crystallites have not previously been imaged in BF in the HBA/HNA copolymers. This failure is thought to be due to the greater radiation damage in the other copolymers, which is sufficient to render the crystallites invisible in the lower contrast conditions typical of BF. As determined from methods outlined in the literature<sup>11–13</sup>, the average saturation doses ( $\mathcal{F}$ ) required for the complete disappearance of crystallites in DF is

between 130–350 C/m<sup>2</sup> for three high-molecular weight ( $DP \approx 150$ ) HBA/HNA copolymers of different compositions and around 430 C/m<sup>2</sup> for a low molecular weight ( $DP \approx 25$ ) 75/25 copolymer. This assumes an ideal screen collection efficiency, thereby providing an underestimate of the effective  $\mathcal{F}$ . The value of  $\mathcal{F}$  measured for the N-AT copolymer is comparable to that recorded for the low molecular weight HBA/HNA material, being  $470 \pm 50$  C/m<sup>2</sup>. Possible reasons for the increased radiation resistance are as follows. The crystalline structure has fewer imperfections than that observed in the high molecular weight HBA/HNA copolymers, and the presence of the aromatic amide stabilizes the copolymer over longer doses. The fact that the crystallites seen in *Figure 4a* diffract more intensely than those in the high molecular weight HBA/HNA copolymers, suggests that there is indeed greater crystalline perfection in this material. Dark entities similar to those seen in *Figure 4b*, have been reported in BF imaging of a lyotropic aromatic amide homopolymer, poly(*p*-phenylene terephthalamide)<sup>14</sup>.

DF imaging along the meridional axis has yielded the micrographs presented in *Figure 5*. *Figure 5a* is obtained by tilting the beam so that the first meridional maximum is centred in the objective aperture (M in *Figure 3*). Diffracting crystallites appear oriented as those observed in *Figure 4a*, with their thin axis parallel to the molecular axis, and measure approximately 15 nm thick and 130 nm long. The good level of orientation (as seen in *Figure 2b*) means that it is exceedingly unlikely that these crystallite images are associated with the wings of the equatorial reflection.

The micrograph shown in *Figure 5b* is acquired by tilting the beam so that the region between the meridional

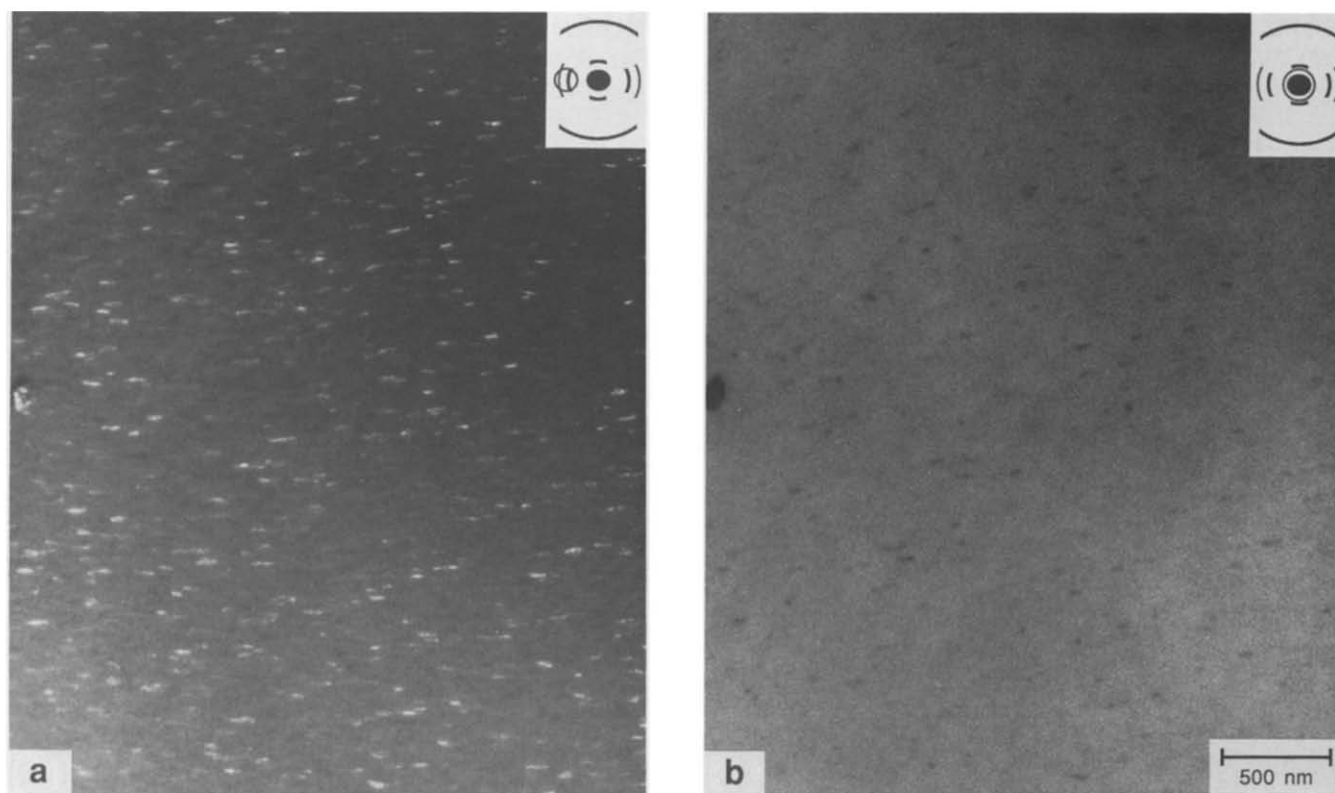


**Figure 4** Coinciding pair of electron micrographs, one obtained in DF using the principal equatorial reflection (a) and the other in BF (b). The DF image (a), obtained first, clearly shows the presence of strongly diffracting crystallites, measuring about 15 nm thick and 90 nm long and oriented with their thin axis parallel to the molecular axis (vertical). The 'dark' entities seen in BF (b) correspond well with the DF crystallites in both size, location, and orientation, despite the effects of radiation damage. The contamination spot (left) is a reference point to facilitate comparison

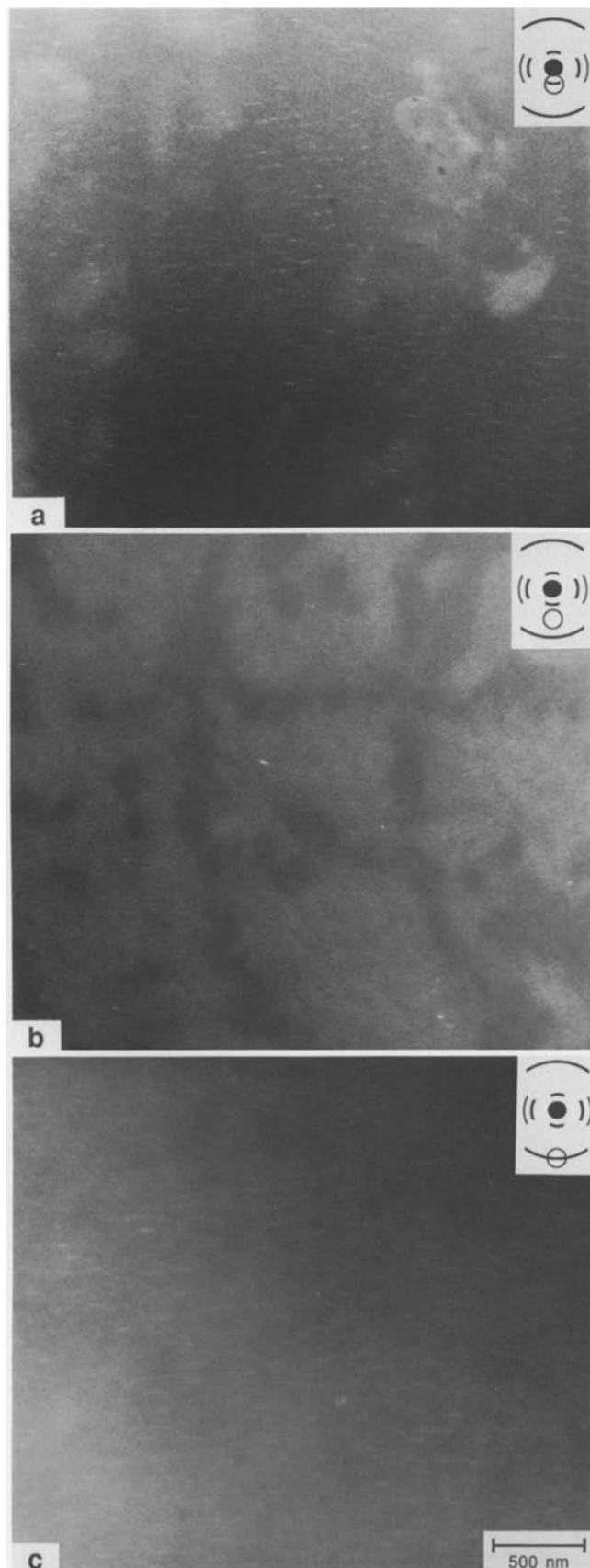


**Figure 5** Series of DF micrographs obtained from different positions along the meridional axis of the SAED: (a) from the first meridional maximum (M in Figure 3), (b) from the intrachain region (I), and (c) from the broad meridional arc (A). Crystallites, oriented the same as in Figure 4 and measuring 15 nm thick and between 130–150 nm long, are clearly evident in (a) and (c), indicating that sharp crystallite imaging is possible only from diffraction peaks. Fine, non-diffracting structure is evident in (b). The extent of contrast-enhancement of the micrographs is discussed in the text. As before, the molecular axis is vertical.

maxima is used as the source of diffraction contrast (I in Figure 3). The discrete crystallites seen in the previous micrographs are not as clearly defined, but are just visible as fine, dark entities (they diffract out of the objective aperture). The larger scale pattern of contrast, also recorded<sup>1</sup> for HBA/HNA materials, remains unexplained at the present.

Centring the outer meridional arc (A in Figure 3) in the objective aperture of the microscope produces the DF image shown in Figure 5c. Although the contrast level is low, distinct diffracting entities are again evident. They measure approximately 15 nm thick and 150 nm long and are oriented as the crystallites seen in previous micrographs. Crystallite imaging in the broader meridional arc has been accomplished in a low molecular weight HBA/HNA copolymer<sup>7</sup> but never before in any of the high molecular weight analogues.

It must be borne in mind that the DF micrographs presented in Figures 5a–c have been contrast enhanced to facilitate the viewing of low contrast structure. To quantify the extent of enhancement, measurement of optical densities of diffracting and background regions in Figure 4b reveals that the average intensity of the crystallites exceeds that of the background by approximately 24%. In the case of Figures 5a, b and c, the corresponding values are estimated to be about 6%, 12% and 10%, respectively.

#### Crystallite characteristics

An enlarged region displaying the morphology of the crystallites is given in Figure 6. The image in Figure 6a is produced from a digitized DF micrograph imaged in the principal equatorial reflection (as in Figure 4a). A high pass filter, averaging pixel intensities over a 50 × 50 array, was used to minimize gradual variations in background intensity. The irregular boundaries of the plate-like crystallites are seen both in Figure 6a and in the corresponding contour map in Figure 6b. The marked irregularity of the top and bottom surfaces, observed in all micrographs (image processed or not), is an expected feature of NPL crystallites and is in accord with the predictions of the statistical modelling reported in ref. 15. 'Dark' regions in Figure 6a appearing the same size and possessing the same orientation as the diffracting crystallites have been observed in a low molecular weight HBA/HNA copolymer<sup>1,7</sup> and represent crystallites that are diffracting outside the objective aperture.

The effect of tilting a specimen 33° about a single-tilt axis nearly normal to the molecular axis and again imaging in the principal equatorial reflection is shown in Figure 7. The apparent increase in the crystallite population is due to a vertical foreshortening of the sample. Here, the entities appear about 30 nm thick and 90 nm long. These measurements would imply that the crystallites are platelets with a size normal to the film in the approximate range 30–40 nm. The fact that this is about half their observed length in the plane of the micrograph may imply that development normal to the film is limited by the surfaces, since the film thickness is approximately 50–100 nm.

#### CONCLUSIONS

Non-periodic layer (NPL) crystallites have been observed in a thermotropic copoly(ester-amide), closely related to

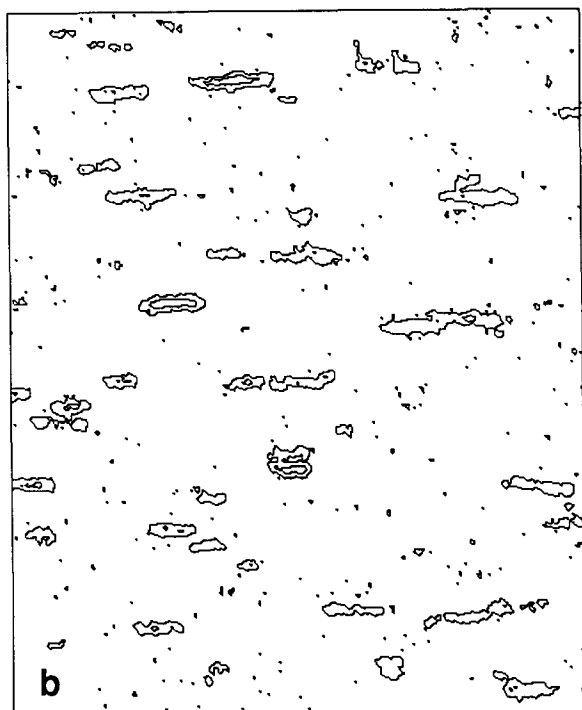
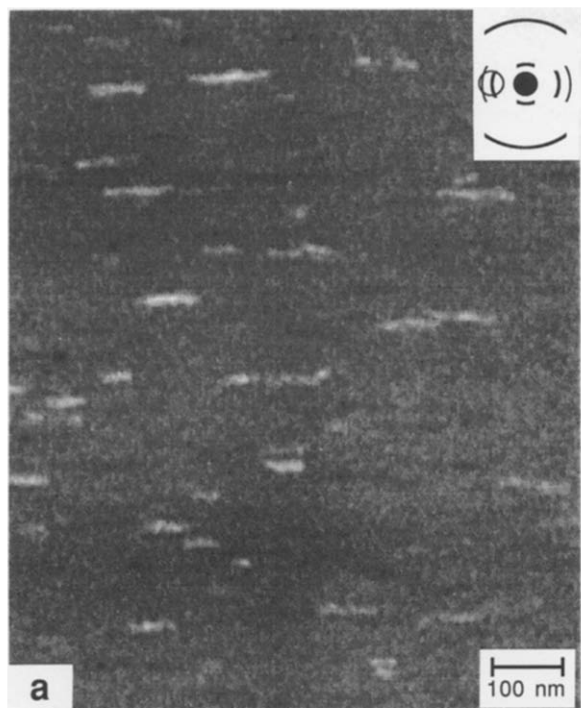


**Figure 6** Close up of some NPL crystallites imaged in the equatorial reflection. The photograph in (a) is a digitized image with a high-pass filter applied to reduce background intensity variations. The corresponding contour map (b) demonstrates the irregularity of the crystallite boundaries

the well-documented HBA/HNA materials. Electron diffraction patterns indicate that the meridional maxima are aperiodic, meaning that the copolymer is random, and that the material becomes highly oriented upon annealing in the solid state. The crystalline structures are plate-like, measuring approximately 15 nm thick and 90 nm long, and are clearly imaged in BF and in DF using the equatorial and meridional reflections as sources of diffraction contrast. Crystallite imaging in the meridional maxima is a result of intensely diffracting crystalline



**Figure 7** DF micrograph of a region tilted  $33^\circ$  along a single-tilt axis nearly parallel to the crystallite axis. Imaging is performed in the principal equatorial reflection, and the shear direction (i.e. molecular axis<sup>11</sup>) is vertical

structures and a marginally greater resistance to beam damage ( $\langle \mathcal{F} \rangle \approx 470 \text{ C/m}^2$ ) as compared to HBA/HNA copolymers. The fact that crystalline entities can be imaged in aperiodic meridional diffraction maxima is significant of their NPL morphology.

#### ACKNOWLEDGEMENTS

Sincere gratitude is expressed towards Professor A. Howie and the Microstructural Physics Group (Cavendish Laboratory) for the use of the electron microscope, J. Mooney for the mass spectroscopy, and Ms L. Sawyer and Dr W. Stobbs for helpful discussions.

#### REFERENCES

- 1 Spontak, R. J. and Windle, A. J. *J. Mater. Sci.*, in press
- 2 Mitchell, G. R. and Windle, A. H. *Colloid Polym. Sci.* 1985, **263**, 230
- 3 Chivers, R. A., Blackwell, J. and Gutierrez, G. A. *Polymer* 1984, **25**, 435
- 4 Blackwell, J., Biswas, A. and Bonart, R. C. *Macromolecules* 1985, **18**, 2126
- 5 Blackwell, J. and Gutierrez, G. *Polymer* 1982, **23**, 671
- 6 Donald, A. M. and Windle, A. H. *J. Mater. Sci. Lett.* 1985, **4**, 58
- 7 Spontak, R. J., Lemmon, T. J. and Windle, A. H., submitted to *Liquid Crystals*
- 8 Lemmon, T. J., Hanna, S. and Windle, A. H. *Polym. Commun.* 1989, **30**, 2
- 9 Windle, A. H., Viney, C., Golombok, R., Donald, A. M. and Mitchell, G. R. *Faraday Discuss. Chem. Soc.* 1985, **79**, 55
- 10 Viney, C., Donald, A. M. and Windle, A. H. *Polymer* 1985, **26**, 870

*Electron microscopy of NPL crystallites: R. J. Spontak and A. H. Windle*

- |    |  |    |   |
|----|--|----|---|
| 11 | Sawyer, L. C. and Grubb, D. T. 'Polymer Microscopy', Chapman and Hall, London, 1987, p. 62   | 13 | Grubb, D. T. <i>J. Mater. Sci.</i> 1974, <b>9</b> , 1715  |
| 12 | Reimer, L. 'Transmission Electron Microscopy: Physics of Image Formation and Microanalysis', Springer-Verlag, New York, 1984, p. 429 | 14 | Dobb, M. G., Johnson, D. J. and Saville, B. P. <i>J. Polym. Sci. Polym. Symp.</i> 1977, <b>58</b> , 237 |
|    |  | 15 | Hanna, S. and Windle, A. H. <i>Polymer</i> 1988, <b>29</b> , 207  |